Stabilizing effect of driving and dissipation on quantum metastable states

Davide Valenti,[1,2] Angelo Carollo,[1] and Bernardo Spagnolo[1,3,4]

[1]*Dipartimento di Fisica e Chimica, Group of Interdisciplinary Theoretical Physics, Università di Palermo and CNISM, Unità di Palermo, Viale delle Scienze, Edificio 18, I-90128 Palermo, Italy*

[2]*Istituto di Biomedicina ed Immunologia Molecolare (IBIM) "Alberto Monroy," CNR, Via Ugo La Malfa 153, I-90146 Palermo, Italy*

[3]*Istituto Nazionale di Fisica Nucleare, Sezione di Catania, Via S. Sofia 64, 95123 Catania, Italy*

[4]*Radiophysics Department, Lobachevsky State University of Nizhni Novgorod, Gagarin ave. 23, 603950 Nizhni Novgorod, Russia*

(Received 7 October 2017; published 13 April 2018)

We investigate how the combined effects of strong Ohmic dissipation and monochromatic driving affect the stability of a quantum system with a metastable state. We find that, by increasing the coupling with the environment, the escape time makes a transition from a regime in which it is substantially controlled by the driving, displaying resonant peaks and dips, to a regime of frequency-independent escape time with a peak followed by a steep falloff. The escape time from the metastable state has a nonmonotonic behavior as a function of the thermal-bath coupling, the temperature, and the frequency of the driving. The quantum noise-enhanced stability phenomenon is observed in the investigated system.

DOI: 10.1103/PhysRevA.97.042109

I. INTRODUCTION

The study of the decay of metastable states has a long-standing tradition in classical and quantum physics [1–3]. In the quantum regime, calculations have been performed based on the imaginary-time path-integral technique [2,4,5] considering a quantum particle initially in a thermal state inside the metastable well. The decay from the metastable state occurs on a time scale that depends on the friction and temperature, and, in the quantum regime, this time scale is essentially determined by tunneling through the potential barrier [5].

Path-integral calculations were initiated from the seminal work by Caldeira and Leggett on the tunneling rate in superconducting devices [6]. There, the authors use imaginary-time path integrals for solving the dissipative quantum decay problem. Real-time path integrals for tunneling problems were used later by Ueda, Bruinsma, and Bak [7]. The real-time approach allows for capturing the dynamics of the particle in terms of populations of spatially localized states in bistable potentials, also in the presence of driving [8–10].

At present, there is significant interest in analyzing metastability and the role of dissipation in open quantum systems [11–14]. Specifically, very recent investigations are aimed at understanding the fundamental aspects of metastability in open quantum systems [15], the metastability in the driven-dissipative Rabi model [16], the energy exchange in a driven open quantum system strongly coupled to a heat bath [17], the high-frequency behavior of periodically driven systems [18], the dissipative stabilization of entanglement in superconducting qubits [19], and the resonant activation phenomenon in a quantum dissipative symmetric two-state system [20].

In Ref. [13], the escape dynamics starting from a nonequilibrium initial condition was investigated for a static potential using the techniques introduced in Ref. [9]. Specifically, in that work it was found that, upon varying the strength γ of the coupling between the particle and an Ohmic environment, the escape time from a quantum metastable state exhibits a nonmonotonic behavior, where the presence of a maximum constitutes a quantum version of the noise-enhanced stability (NES) phenomenon, theoretically and experimentally well investigated in Refs. [21–27], called quantum noise-enhanced stability [13]. The results obtained there rely on an initial condition substantially different from the quasiequilibrium state inside the metastable well. The preparation was indeed assumed to be such that the particle is initially in a nonequilibrium position between the top of the barrier and the so-called *exit point* of the potential (see Fig. 1 and Refs. [10,23]).

In the present investigation, we analyze the role of driving in the escape from quantum metastable states in the presence of dissipation. We find that the escape time, as a function of the frequency of monochromatic driving with suitable amplitude, displays resonant peaks and dips in the lower part of the range of γ considered. At stronger coupling, the escape time has a maximum, followed by a steep reduction at a critical value of the coupling. This marks the transition to a frequency-independent behavior that essentially resembles that of the static case.

II. MODEL

The archetype of a quantum dissipative system is provided by the Caldeira-Leggett model [28], where a central system (S) of generalized coordinate $\hat{x}$ is coupled to a dissipative environment, a heat bath of quantum harmonic oscillators of frequencies ω_j and coordinates $\hat{x}_j$, according to the Hamiltonian

$$\hat{H}(t) = \hat{H}_S(t) + \frac{1}{2}\sum_{j=1}^{N}\left[\frac{\hat{p}_j^2}{m_j} + m_j\omega_j^2\left(\hat{x}_j - \frac{c_j}{m_j\omega_j^2}\hat{x}\right)^2\right]. \tag{1}$$

The time dependence in H_S accounts for the presence of a time-varying potential which drives the particle. The second

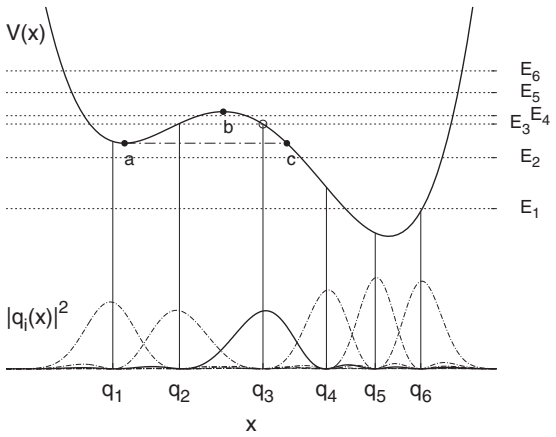

FIG. 1. Potential V [Eq. (3), with $\Delta U = 1.4\hbar\omega_0$ and $\epsilon = 0.27\sqrt{M\hbar\omega_0^3}$] and the first six energy levels (horizontal lines). In the lower part, the probability densities $|q_i(x)|^2 = |\langle x|q_i\rangle|^2$ associated with the DVR eigenfunctions are shown, the initial state $|q_3\rangle$ being highlighted by a solid line. Vertical lines indicate the position eigenvalues in the DVR. The *metastable region* of the potential is to the left of the so-called *exit point c*.

term on the right-hand side of Eq. (1) contains the free bath Hamiltonian, the (bilinear) interaction term between S and the oscillators, and a renormalization term, dependent on $\hat{x}^2$, which gives a purely dissipative bath, i.e., a coordinate-independent dissipation for the central system.

The open system S in the present work is a quantum particle of effective mass M subject to a static double-well potential and driven by a monochromatic field of amplitude A and angular frequency Ω. The resulting time-dependent Hamiltonian for S reads

$$\begin{aligned}\hat{H}_S(t) &= \frac{\hat{p}^2}{2M} + V(\hat{x}) - \hat{x}A\sin(\Omega t)\\ &= \hat{H}_0 - \hat{x}A\sin(\Omega t).\end{aligned} \tag{2}$$

The static potential is parametrized by the quartic function of the particle's coordinate $\hat{x}$,

$$V(\hat{x}) = \frac{M^2\omega_0^4}{64\Delta U}\hat{x}^4 - \frac{M\omega_0^2}{4}\hat{x}^2 - \epsilon\hat{x}. \tag{3}$$

Here ω_0 is the oscillation frequency around the potential minima, ϵ is a static bias, and ΔU is the barrier height at zero bias. Throughout the present work, we scale all the physical quantities with ω_0, which is of the same order of magnitude of the frequency spacing between the ground state and the first excited energy level. We choose ϵ sufficiently large to get a configuration that, in the transient dynamics, is suitable for modeling the decay in a metastable potential, starting from a nonequilibrium condition. In the upper part of Fig. 1, $V(x)$ is shown for $\Delta U = 1.4\hbar\omega_0$ and $\epsilon = 0.27\sqrt{M\hbar\omega_0^3}$.

By considering a thermal equilibrium bath, its influence on the quantum bistable system is fully characterized by the spectral density, whose general expression is [10,29]

$$J(\omega) = \frac{\pi}{2}\sum_{j=1}^{N}\frac{c_j^2}{m_j\omega_j}\delta(\omega-\omega_j). \tag{4}$$

For a set of discrete modes, the spectral density consists of a sequence of δ peaks. To work with a genuine heat bath, we assume that the eigenfrequencies ω_j are so dense as to form a continuous spectrum. In the continuum limit, $J(\omega)$ becomes a smooth function of ω, and the sum in Eq. (4) is replaced by an integral. In particular, if the jth coupling coefficient is given by

$$c_j = \left(\gamma\frac{2Mm_j}{\pi j}\omega_j^3\right)^{1/2}, \tag{5}$$

then, substituting Eq. (5) in Eq. (4), with $\omega_j/j = \Delta\omega_j$, we get

$$\begin{aligned}J(\omega) &= M\gamma\sum_{j=1}^{N}\Delta\omega_j\omega_j\delta(\omega-\omega_j)\\ &\xrightarrow{N\gg1} M\gamma\int_0^\infty d\omega'\omega'\delta(\omega-\omega') = M\gamma\omega,\end{aligned} \tag{6}$$

obtaining the Ohmic spectral density in the continuous limit. Equations (5) and (6) show that, if the environment is a large collection of oscillators, one can have strong dissipation, quantified by γ, and still a weak coupling with the individual oscillators [10,29].

However, allowing this linear behavior [Eq. (6)] to persist for an arbitrarily high frequency gives nonphysical results such as, for example, the divergence of the renormalization term in the Hamiltonian (1) (see Refs. [10,28,29]). We then consider, for the dissipative environment, the Ohmic spectral density function J with a high-frequency cutoff. In the continuum limit, we have then [10,13,29]

$$J(\omega) = M\gamma\omega e^{-\omega/\omega_c}, \tag{7}$$

where ω_c is the cutoff frequency of the environment. This cutoff frequency is chosen in such a way as to be much larger than all the other frequencies involved in the dynamics, that is, ω_0 and the frequencies corresponding to jumps between different energy levels of the static potential (see Fig. 1). We set this cutoff frequency to the value $\omega_c = 10\omega_0$. The generalized Langevin equation for the system described by Hamiltonian (1) for an Ohmic bath has a memoryless friction kernel with friction coefficient γ [10]. This coefficient, which has the dimension of a frequency, provides a measure of the overall coupling between S and the heat bath, whereas the couplings with the individual bath oscillators are given by the coefficients c_j (5) in Eq. (1).

A. Discrete variable representation

At low temperatures, on the energy scale set by ω_0, the time evolution of the particle is practically confined to a reduced Hilbert space spanned by the first M energy eigenstates $|E_i\rangle$, provided that the particle is not initially excited to energy levels higher than M. We assume furthermore that the time-dependent driving does not excite further energy eigenstates with respect to those used in the static potential. Moreover, the energy eigenstates are the same as for the system defined by $\hat{H}_0$ in Eq. (2). In addition, when the frequency of the periodic external driving is of the order of the frequency associated with the frequency spacing between the ground state and the first excited energy level or larger, $\Omega \gtrsim \omega_0$, the averaging of

the dynamics over a full driving period is appropriate [8,9]. After averaging, the resulting transition coefficients become time-independent (see the next section), forming the time-averaged rate matrix. Outside of this high-frequency driving assumption, as an alternative theoretical technique, the Floquet theory should be used.

In Fig. 1, the $M = 6$ case is explicitly shown for the strongly asymmetric potential used throughout the present work. In this truncated Hilbert space, we perform the unitary transformation T, which diagonalizes the position operator $\hat{x}$ according to

$$\begin{aligned}\mathbf{q}^{\mathrm{DVR}} &= \mathbf{T}\mathbf{x}\mathbf{T}^{\dagger} \\ &= \mathrm{diag}\{q_1,\ldots,q_M\},\end{aligned} \tag{8}$$

where $\mathbf{x}$ is the matrix representing $\hat{x}$ in the energy basis. The resulting states are

$$|q_j\rangle = \sum_{k=1}^{M} T_{jk}^{*}|E_k\rangle, \tag{9}$$

where $T_{ij} = (\mathbf{T})_{ij}$ satisfy the eigenvalue equation $q^{\mathrm{DVR}}|q_j\rangle = q_j|q_j\rangle$.

The set $\{(q_j,|q_j\rangle), \quad j = 1,\ldots,M\}$ constitutes the so-called discrete variable representation (DVR) [30,31]. We consider the bath in the thermal state and a factorized initial condition $\rho(t_0)\bigotimes\rho_B(0)$ is set, with $\rho_B(0) = e^{-\beta\hat{H}_B}/Z_B$. The particle's reduced density operator in the DVR is given by

$$\rho_{\mu\nu}(t) = \sum_{\alpha,\beta=1}^{6} K(q_\mu,q_\nu,t;q_\alpha,q_\beta,0)\rho_{\alpha\beta}(0), \tag{10}$$

where $\rho_{\mu\nu}(t) = \langle q_\mu|\rho(t)|q_\nu\rangle$ $(\mu,\nu = 1,\ldots,6)$ and the propagator $K(q_\mu,q_\nu,t;q_\alpha,q_\beta,0)$ is given by the double dissipative path integral,

$$\int_{q_\alpha}^{q_\mu}\mathcal{D}q(t)\int_{q_\beta}^{q_\nu}\mathcal{D}^{*}q'(t)\mathcal{A}[q]\mathcal{A}^{*}[q']\,\mathcal{F}_{\mathrm{FV}}[q,q']. \tag{11}$$

Here $\mathcal{A}[q]$ is the amplitude associated with the path $q(t)$ of the bare system. The effect exerted by the bath on the quantum-mechanical amplitude associated with a path $(q(t),q'(t))$ is condensed in the Feynman-Vernon (FV) influence functional $\mathcal{F}_{\mathrm{FV}}[q,q']$ [32].

This approach is nonperturbative in the system-bath coupling, and is thus suited for dealing with the strong-coupling regime. The functions $q_j(x) = \langle x|q_j\rangle$ are *localized* around the eigenvalues q_j, as can be seen in the lower part of Fig. 1: the particle in the jth DVR state has a nonvanishing probability of being detected only in a spatial region centered around q_j. This spatially discretized picture generalizes the localized representation for a two-state system, given in terms of left or right states localized around the potential minima [10]. The DVR allows for calculating the probability of finding the particle in the region in-between the minima. In the present work, we exploit this possibility of studying the transient dynamics in terms of escape time towards the lower well, starting from a nonequilibrium initial state (see the lower part of Fig. 1). Note that spatial continuity is recovered for $M \to \infty$, i.e., removing the upper bound on the energies taken into account. The existence of intermediate localized states in the generalization of the two-state system treatment accomplished by the DVR is reflected by the multiple time scales resulting from the inclusion of energy levels above the first doublet and accounts for tunneling and intrawell relaxation [9,33].

III. STRONG DISSIPATION AND HIGH-FREQUENCY DRIVING: ANALYTICAL APPROACH

In the DVR representation, a path consists of a sequence of transitions in the spatial grid defined by the set $\{q_1,\ldots,q_6\}$ so that the double path integral (11) turns into a sum over all the possible discrete paths $\{\mu_j,\nu_j = 1,\ldots,6\}$ [9,10,29]. As a further approximation, in addition to the use of a limited set of DVR, in the propagator $K(q_\mu,q_\nu,t;q_\alpha,q_\beta,0)$ we restrict the sum over paths to the leading contributions. These are given by the class of paths consisting in sojourns in diagonal states, that is, the time intervals in which the system is in a diagonal state of the reduced matrix, interrupted by single off-diagonal excursions called *blips*. In the dissipation regimes from intermediate to high temperature, on the scale fixed by $\hbar\omega_0$, considered here, the nonlocal-in-time interactions among different blips can be neglected. This corresponds to a multilevel version [9,29,33] of the *noninteracting blip approximation* (NIBA) [10,34]. However, the relevant part of the interactions, i.e., the intrablip interactions, is retained to all orders in the coupling strength. This is the content of the generalized *noninteracting cluster approximation* (gNICA) [9], where a *cluster* is defined as the time interval during which the path visits nondiagonal elements. The gNICA is therefore the generalization to a multilevel system of the NIBA applicable for a spin-boson system [9].

In the framework of the gNICA, the double path integral of Eq. (11) assumes a factorized form in the Laplace space, allowing for the derivation of a generalized master equation

$$\dot{\rho}_{jj}(t) = \sum_k \int_{t_0}^{t} dt' K_{jk}(t,t')\rho_{kk}(t'). \tag{12}$$

At strong damping, as in our case, the memory time of the kernels K_{jk} is smaller than the characteristic time scale of the evolution of populations. In other words, in the short-time interval in which K_{jk} are substantially different from zero, $\rho_{kk}(t)$ are practically constant. Under the assumption called the *Markovian approximation*, in which $\rho_{kk}(t')$ in (12) are practically constant on the timescales at which the kernels K_{jk} are significantly different from zero, we can put $\rho_{kk}(t')$ outside the integral and bring the upper limit to ∞. Setting $t_0 = 0$, the time-dependent rates are thus given by

$$\Gamma_{jk}(t) = \int_0^{\infty} d\tau\, K_{jk}(t,t-\tau), \tag{13}$$

where $\tau = t - t'$. In the presence of a time-dependent driving, the kernels no longer depend only on the difference τ, and consequently the integration over τ leaves us with time-dependent rates. However, if the frequency Ω of the monochromatic driving is sufficiently high so that it does not match any of the system's frequencies (renormalized by the bath), the average over one period $\mathcal{T} = 2\pi/\Omega$ can be taken [8,9], which gives the following time-independent averaged rates:

$$\Gamma_{jk}^{av} = \frac{\Omega}{2\pi}\int_0^{\frac{2\pi}{\Omega}} dt \int_0^{\infty} d\tau\, K_{jk}(t,t-\tau). \tag{14}$$

The populations ρ_{jj} of the DVR states $|q_j\rangle$ undergo a relaxation towards a stationary configuration, which depends on bath parameters and the damping strength γ. Therefore, at strong coupling this process is well approximated by the incoherent relaxation captured by the master equation [9,29]

$$\dot{\rho}_{jj}(t) = \sum_k \Gamma^{\rm av}_{jk}\rho_{kk}(t), \tag{15}$$

with $\Gamma^{\rm av}_{jk}$ given by Eq. (14). The kernel elements K_{jk} are taken to the second order in the transition amplitudes per unit time Δ_{jk} and at all orders in the system-bath coupling. They go to zero exponentially due to the presence of a cutoff. For $j \neq k$, the kernels read

$$K_{jk}(t,t') = 2\Delta^2_{jk} e^{-q^2_{jk}Q'(t-t')} \times \cos\left[\zeta_{jk}(t,t') + q^2_{jk}Q''(t-t')\right], \tag{16}$$

with the diagonal elements of the kernel matrix given by

$$K_{kk}(t,t') = -\sum_{n\neq k} K_{nk}(t,t'), \tag{17}$$

according to the conservation of probability. In Eq. (16), the matrix elements Δ_{jk} are given by

$$\Delta_{jk} \equiv \langle q_j|\hat{H}_0|q_k\rangle/\hbar, \tag{18}$$

$q_{jk} = q_j - q_k$, and the functions $\zeta_{jk}(t,t')$ are defined as the time integrals

$$\zeta_{jk}(t,t') = \int_{t'}^{t} dt''\left[(\Delta_{jj} - \Delta_{kk}) - q_{jk}(A/\hbar)\sin(\Omega t'')\right]. \tag{19}$$

Finally, in Eq. (16), Q' and Q'' are, respectively, the real and imaginary parts of the function $Q(t)$, related to the bath correlation function $L(t)$ by $L(t) = \hbar^2 d^2 Q(t)/dt^2$. In the scaling limit set by $k_B T/\hbar\omega_c \ll 1$, we have [29]

$$\begin{aligned} Q(t) &= Q'(t) + iQ''(t) \\ &= \frac{M\gamma}{\pi\hbar}\ln\left(\sqrt{1+\omega_c^2 t^2}\,\frac{\sinh(\kappa t)}{\kappa t}\right) \\ &\quad + i\frac{M\gamma}{\pi\hbar}\arctan(\omega_c t), \end{aligned} \tag{20}$$

where $\kappa = \pi k_B T/\hbar$.

The master equation (15), with rates given by Eq. (14), describes the average effect of the high-frequency driving on the time evolution of the populations ρ_{jj} of the DVR states. The analytical solution of Eq. (15) reads

$$\rho_{jj}(t) = \sum_{n,k=1}^{M} S_{jn}(S^{-1})_{nk} e^{\Lambda_n(t-t_0)}\rho_{kk}(t_0), \tag{21}$$

where $\mathbf{S}$ is the transformation matrix diagonalizing the rate matrix Γ, which has eigenvalues Λ_n. The smallest, in absolute value, of the nonzero eigenvalues determines the largest timescale of the dynamics, the quantum relaxation time $\tau_{\rm relax}$ [9].

IV. ESCAPE TIME FOR THE DRIVEN SYSTEM

We analyze the transient dynamics of the driven system by Eq. (21) with the nonequilibrium initial condition

$$\rho(0) = |q_3\rangle\langle q_3|, \tag{22}$$

that is, with the particle initially prepared in the central region of the potential on the right side of the barrier, between the maximum and the *exit point*, denoted by c in Fig. 1. Therefore, the dynamical evolution of the populations of our asymmetric bistable quantum system (see Fig. 1) with the initial condition (22) is given by

$$\rho_{jj}(t) = \sum_{n=1}^{6} S_{jn}(S^{-1})_{n3} e^{\Lambda_n(t-t_0)}\rho_{33}(t_0). \tag{23}$$

We consider the escape time from the *metastable region*, defined as the region to the left of the *exit point* (c in Fig. 1), according to Ref. [35]. There, the decay rate from the metastable region is calculated by using the probability of penetration of the Gaussian wave packet from left to right through the potential barrier of Fig. 1. Here, we use a discretized version of this theoretical technique. Therefore, we calculate the population of the lower (right side) well, that is, the cumulative population of the three DVR states from $|q_4\rangle$ to $|q_6\rangle$,

$$P_{\rm right}(t) = \sum_{j=4}^{6}\rho_{jj}(t). \tag{24}$$

During the transient dynamics, the cumulative population of the metastable well, $|q_1\rangle$ and $|q_2\rangle$, reaches a maximum, and then, by tunneling through the potential barrier, decays finally settling down to a stationary value dependent on the temperature. We define the escape time τ from the metastable region of the potential (the region to the left of the exit point c) as the time the right well population takes to cross a threshold value d. The nonmonotonic behavior of τ as a function of γ and of the temperature T predicted in the static case was shown in Ref. [13] to be robust against variations of the threshold around the value 0.9.

Here we set the threshold at $d = 0.95$, meaning that we consider the particle that escaped from the metastable region when the probability to detect it in the lower (right) well is equal to or greater than 95%. Note that, due to the incoherent relaxation described by Eq. (21), once the threshold is crossed no oscillatory behavior of the populations occurs (no recrossing of the threshold in the opposite direction). Therefore, if the particle crosses the threshold at time τ, the overall population of the metastable region is not going to be larger than 0.05 at later times.

At this point we note that, in the static case, the metastable well can be thermally populated at the steady state. In this scenario, no escape can occur if the threshold d is close to unit [13]. As we show in what follows, the same is true in the driven case for certain values of the frequency Ω, especially at large amplitudes A, whenever the left well population, namely the sum $P_{\rm left} = \rho_{11} + \rho_{22}$, is kept substantially above zero at the steady state by the presence of the driving. An example of this effect is given in Fig. 2, where for $\bar{A} = 0.15$, $\bar{T} = 0.1$, and $\gamma/\omega_0 = 0.2$, the left well population is plotted against time for different driving frequencies. Here we introduced the

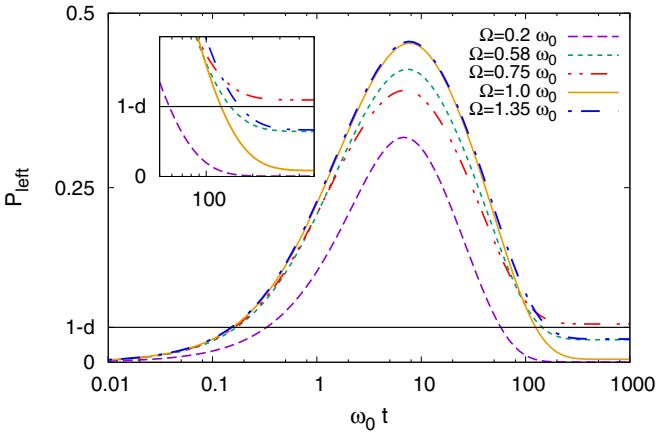

FIG. 2. Left well population $P_{\text{left}} = \rho_{11} + \rho_{22}$ as a function of time (in log scale) for $\bar{A} = 0.15$, $\bar{T} = 0.1$, $\gamma/\omega_0 = 0.2$, and five driving frequency values, namely $\Omega/\omega_0 = 0.2, 0.58, 0.75, 1.0, 1.35$. Here we introduced the dimensionless quantities of the amplitude and temperature, $\bar{A} = A/\sqrt{M\hbar\omega_0^3}$ and $\bar{T} = k_B T/\hbar\omega_0$. Horizontal line: $1 - d$, where $d = 0.95$ is the threshold value. For $\Omega/\omega_0 = 0.75$ no escape occurs, as P_{left} remains above the value $1 - d$. This is better shown in the inset. Note the nonmonotonic behavior of the steady-state values of P_{left} as a function of Ω.

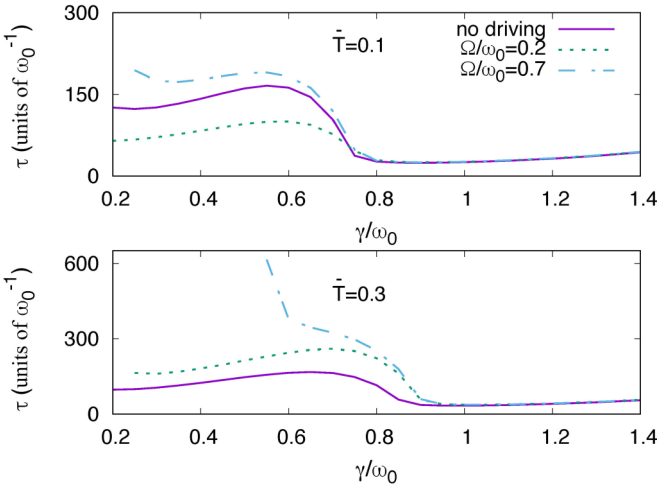

FIG. 3. Escape time vs coupling strength for three driving settings, namely $\Omega/\omega_0 = 0, 0.2, 0.7$. Upper panel: dimensionless temperature $\bar{T} = 0.1$. At $\Omega/\omega_0 = 0.7$, no escape occurs for $\gamma/\omega_0 \lesssim 0.25$. Lower panel: dimensionless temperature $\bar{T} = 0.3$. For $\Omega/\omega_0 = 0.2$ and $\Omega/\omega_0 = 0.7$, the escape occurs starting from $\gamma/\omega_0 \lesssim 0.25$ and 0.55, respectively. For both panels, the driving dimensionless amplitude is fixed at the value $\bar{A} = 0.15$. Solid lines, in both panels, give the behavior in the absence of driving $\Omega = 0$.

dimensionless quantities of the amplitude and temperature, $\bar{A} = A/\sqrt{M\hbar\omega_0^3}$ and $\bar{T} = k_B T/\hbar\omega_0$. The stationary value of P_{left} is above $1 - d = 0.05$ for $\Omega/\omega_0 = 0.75$, meaning that the escape does not occur at this driving frequency.

V. RESULTS AND DISCUSSION

In the absence of external driving, $A = 0$, as γ increases, both the escape time τ and the relaxation time τ_{relax} increase [13]. This holds until a critical value of γ_c, dependent on the temperature, is reached: by further increasing γ, the escape time steeply diminishes whereas the relaxation time continues to increase monotonically. In Fig. 3, the behavior of the escape time τ versus γ/ω_0 for three values of frequency, namely $\Omega/\omega_0 = 0, 0.2, 0.7$, and two different temperatures, that is, $\bar{T} = 0.1, 0.3$, is shown. At the lower temperature $\bar{T} = 0.1$, all the curves show a nonmonotonic behavior, with a maximum, of τ as a function of the scaled coupling parameter γ/ω_0. At the higher temperature $\bar{T} = 0.3$, the same behavior occurs for the lower values of the scaled driving frequency $\Omega/\omega_0 = 0, 0.2$, while a monotonic behavior is observed for the higher-frequency value of $\Omega/\omega_0 = 0.7$. This monotonic behavior can be ascribed to the conjunct effect of thermal bath and driving force, which accelerates the escape process from the metastable region by increasing the coupling parameter γ.

The maxima in the escape time imply that, at a given temperature, there is an optimal value of the coupling γ for which the depletion of the metastable region is delayed. According to the well-known classical phenomenon [21–27], we address this feature as quantum noise-enhanced stability (qNES) [13].

Moreover, a critical value of the coupling strength γ_c, dependent on the temperature, exists also in the presence of driving. The critical values of this coupling parameter in Fig. 3 are found to be $\gamma_c/\omega_0 \simeq 0.75$ at $\bar{T} = 0.1$ and $\gamma_c/\omega_0 \simeq 0.9$ at $\bar{T} = 0.3$.

At the higher temperature, for $\Omega/\omega_0 = 0.7$, there is no escape up to $\gamma/\omega_0 \simeq 0.55$. At stronger dissipation the interaction with the heat bath forces the relaxation towards the lower well causing the depletion of the metastable well, which would be otherwise populated due to the combined effect of driving and thermal excitation. We note that γ_c is larger at the higher temperature, indicating that at strong coupling, and in the presence of driving, the thermal excitations of the heat bath contrast the relaxation induced by the bath itself.

An interesting feature, at strong coupling and independently of the driving frequency, is the presence of a slow monotonic increase of the escape time τ for $\gamma/\omega_0 > \gamma_c/\omega_0$, which is a signature of the quantum Zeno effect [36].

Our main focus in this section is the investigation of the escape time as a function of the driving frequency and coupling strength. This is aimed at giving a systematic account for the delay and the quench of the escape shown in Fig. 3, and at investigating how these effects are influenced by variations of the coupling with the environment. Toward that end, first we fix γ at the value used in Fig. 2, the lowest value considered here, and we plot the escape time as a function of Ω for three different values of the dimensionless driving amplitudes $\bar{A}$ (see Fig. 4). Then we show the escape time as a function of Ω and γ for two different values of the dimensionless amplitude $\bar{A}$ (see Figs. 5 and 6).

The plot τ versus Ω, shown in Fig. 4, is characterized by resonant peaks and dips whose magnitude is enhanced by increasing the driving amplitude, the escape being completely quenched for frequencies around $\Omega/\omega_0 \simeq 0.75$ for $A \geqslant 0.15\sqrt{M\hbar\omega_0^3}$. The effect is easily interpreted by looking at Fig. 2, where the case $\Omega/\omega_0 = 0.75$ displays at the steady

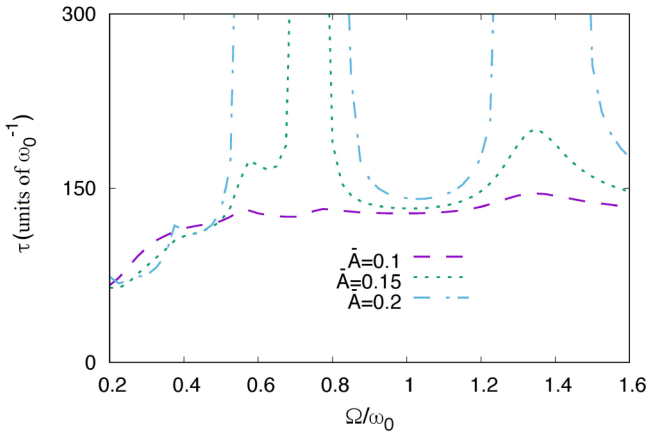

FIG. 4. Escape time vs driving frequency for three values of the dimensionless driving amplitude $\bar{A} = A/\sqrt{M\hbar\omega_0^3}$, namely $\bar{A} = 0.1, 0.15, 0.2$. Other parameters are $\gamma/\omega_0 = 0.2$ and $\bar{T} = 0.1$.

state a left-well population larger than $1 - d$, implying that $P_{\text{right}} < d$. The frequencies for which τ is maximized (or no escape occurs, depending on the amplitude) correspond roughly to the energy separations $E_3 - E_2 \approx 0.6\hbar\omega_0$, $E_4 - E_2 \approx 0.8\hbar\omega_0$, and $E_5 - E_2 \approx 1.25\hbar\omega_0$, showing that a resonance phenomenon between the external driving and these frequencies occurs. For $\Omega \approx \omega_0$, a minimum of τ is visible, which is akin to the quantum resonant activation phenomenon [20].

Peaks and dips in τ as a function of the driving frequency are smoothed out as γ increases until τ becomes practically constant, with respect to Ω, as the coupling approaches the critical value mentioned above. This behavior is displayed in Figs. 5 and 6, where the escape time is plotted as a function of Ω/ω_0 and γ/ω_0 for two values of the amplitude, $\bar{A} = 0.15$ and 0.20, respectively. For $\gamma < \gamma_c$, the high-frequency driving can delay or accelerate the escape, while for coupling strengths above the critical value γ_c the escape time becomes frequency-independent and the quantum Zeno effect occurs [36].

The critical value γ_c marks the transition to a dynamical regime in which the tunneling mechanism of population transfer to the states of the *metastable region* is suppressed. This is because the tunneling dynamics becomes slow on the depletion time scale of the region where the particle is initially prepared. As a result, the probability of detecting the particle

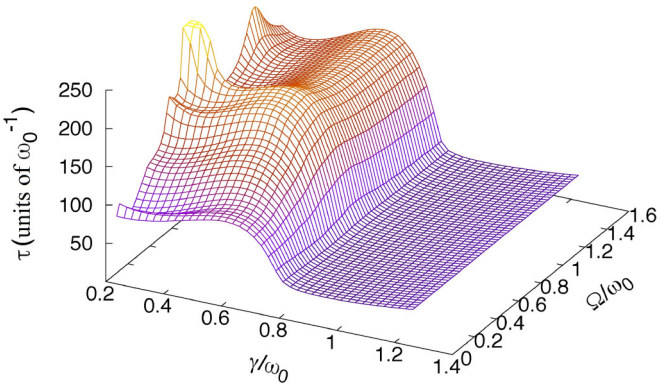

FIG. 5. Escape time as a function of the coupling strength and the driving frequency for dimensionless amplitudes $\bar{A} = 0.15$. The dimensionless temperature is set to the value $\bar{T} = 0.1$.

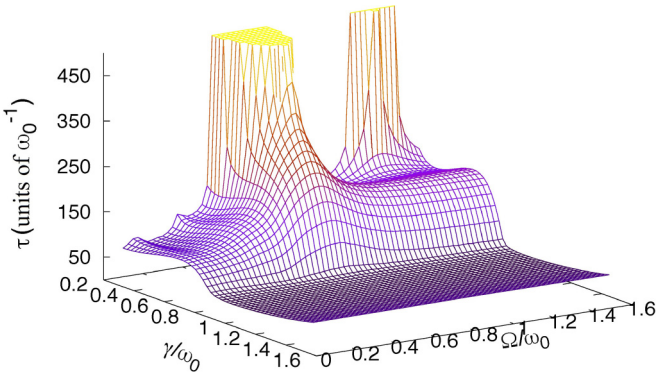

FIG. 6. Escape time as a function of the coupling strength and the driving frequency for dimensionless amplitudes $\bar{A} = 0.20$. The dimensionless temperature is set to the value $\bar{T} = 0.1$.

in the metastable well, starting from the initial condition (22), is practically zero at every time instant as the population is directly transferred from $|q_3\rangle$ to the right well states. This effect is not captured by the relaxation time (see Sec. III), which is independent of the initial condition and grows monotonically as γ increases.

To give an account of this transition, in Fig. 7 we plot the left well population P_{left} as a function of the time at fixed driving frequency (in correspondence of a peak in τ) for three values of γ, below and above $\gamma_c/\omega_0 \simeq 0.75$ (see the upper panel of Fig. 3), namely $\gamma/\omega_0 = 0.2, 0.6, 1.0$. We find that above γ_c almost no population transfer occurs to the left well during the transient dynamics (red dashed-dotted curve).

VI. CONCLUSIONS

In this work, we investigated the transient dynamics of a quantum particle subject to an asymmetric bistable potential in the presence of strong Ohmic dissipation and high-frequency

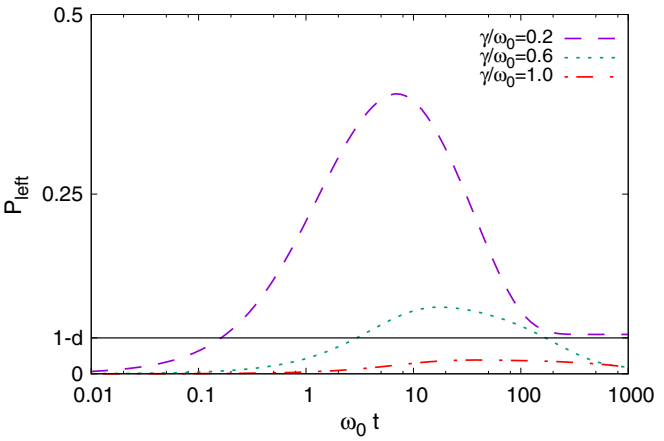

FIG. 7. Left well population $P_{\text{left}} = \rho_{11} + \rho_{22}$ as a function of the time (in log scale), at driving frequency $\Omega/\omega_0 = 0.75$, for three values of the scaled coupling parameter, namely $\gamma/\omega_0 = 0.2$ (magenta dashed line), $\gamma/\omega_0 = 0.6$ (green dotted line), and $\gamma/\omega_0 = 1.0$ (red dashed-dotted line). Parameters are $\bar{A} = 0.15$ and $\bar{T} = 0.1$. Horizontal line: $1 - d$, where $d = 0.95$ is the threshold value. The critical value of the scaled coupling parameter is $\gamma_c/\omega_0 \simeq 0.75$.

driving. This was done by considering the escape time from the *metastable region*, the region to the left of the exit point of the potential (point c in Fig. 1), starting from a nonequilibrium initial condition.

We found that, by tuning the frequency of a monochromatic driving with suitable amplitude at specific values dictated by the shape of the potential, the escape from the metastable region can be slowed down, accelerated, or even inhibited, provided that the coupling strength is smaller than a critical value dependent on the temperature. This marks the transition to a frequency-independent behavior of the escape time.

Quantum noise-enhanced stability is observed in the system investigated. This way of controlling the escape dynamics and the asymptotic population of the metastable well in the strong-coupling regime may be of practical interest, given the possibility of engineering dissipative environments in superconducting devices [37] and exploiting dissipation-induced steady states for quantum computation [38,39].

ACKNOWLEDGMENTS

This work was supported by a Grant of the Government of the Russian Federation (RU) (Contract No. 14.Y26.31.0021). We acknowledge also partial support by Ministry of Education, University and Research (IT).

[1] H. A. Kramers, Physica **7**, 284 (1940).
[2] I. Affleck, Phys. Rev. Lett. **46**, 388 (1981).
[3] P. Hänggi, J. Stat. Phys. **42**, 105 (1986).
[4] H. Grabert, U. Weiss, and P. Hänggi, Phys. Rev. Lett. **52**, 2193 (1984).
[5] H. Grabert, P. Olschowski, and U. Weiss, Phys. Rev. B **36**, 1931 (1987).
[6] A. O. Caldeira and A. J. Leggett, Phys. Rev. Lett. **46**, 211 (1981).
[7] M. Ueda, Phys. Rev. B **54**, 8676 (1996); R. Bruinsma and P. Bak, Phys. Rev. Lett. **56**, 420 (1986).
[8] M. Grifoni and P. Hänggi, Phys. Rep. **304**, 229 (1998).
[9] M. Thorwart, M. Grifoni, and P. Hänggi, Ann. Phys. (N.Y.) **293**, 15 (2001); Phys. Rev. Lett. **85**, 860 (2000).
[10] U. Weiss, *Quantum Dissipative Systems*, 4th ed. (World Scientific, Singapore, 2012).
[11] R. Schmidt, A. Negretti, J. Ankerhold, T. Calarco, and J. T. Stockburger, Phys. Rev. Lett. **107**, 130404 (2011).
[12] M. Abdi, P. Degenfeld-Schonburg, M. Sameti, C. Navarrete-Benlloch, and M. J. Hartmann, Phys. Rev. Lett. **116**, 233604 (2016).
[13] D. Valenti, L. Magazzù, P. Caldara, and B. Spagnolo, Phys. Rev. B **91**, 235412 (2015).
[14] F. Letscher, O. Thomas, T. Niederprüm, M. Fleischhauer, and H. Ott, Phys. Rev. X **7**, 021020 (2017); J. Galego, F. J. Garcia-Vidal, and J. Feist, Phys. Rev. Lett. **119**, 136001 (2017).
[15] K. Macieszczak, M. Guţă, I. Lesanovsky, and J. P. Garrahan, Phys. Rev. Lett. **116**, 240404 (2016).
[16] A. Le Boité, M.-J. Hwang, and M. B. Plenio, Phys. Rev. A **95**, 023829 (2017).
[17] M. Carrega, P. Solinas, M. Sassetti, and U. Weiss, Phys. Rev. Lett. **116**, 240403 (2016).
[18] M. Bukov, L. D'Alessio, and A. Polkovnikov, Adv. Phys. **64**, 139 (2015).
[19] M. E. Kimchi-Schwartz, L. Martin, E. Flurin, C. Aron, M. Kulkarni, H. E. Tureci, and I. Siddiqi, Phys. Rev. Lett. **116**, 240503 (2016).
[20] L. Magazzù, P. Hänggi, B. Spagnolo, and D. Valenti, Phys. Rev. E **95**, 042104 (2017).
[21] R. N. Mantegna and B. Spagnolo, Phys. Rev. Lett. **76**, 563 (1996).
[22] A. A. Dubkov, N. V. Agudov, and B. Spagnolo, Phys. Rev. E **69**, 061103 (2004).
[23] A. Fiasconaro, J. J. Mazo, and B. Spagnolo, Phys. Rev. E **82**, 041120 (2010).
[24] N. V. Agudov and A. N. Malakhov, Phys. Rev. E **60**, 6333 (1999); D. Dan, M. C. Mahato, and A. M. Jayannavar, *ibid.* **60**, 6421 (1999); R. Wackerbauer, *ibid.* **59**, 2872 (1999); A. Mielke, Phys. Rev. Lett. **84**, 818 (2000).
[25] A. L. Pankratov and B. Spagnolo, Phys. Rev. Lett. **93**, 177001 (2004); P. D'Odorico, F. Laio, and L. Ridolfi, Proc. Natl. Acad. Sci. (U.S.A.) **102**, 10819 (2005); G. Bonanno, D. Valenti, and B. Spagnolo, Eur. Phys. J. B **53**, 405 (2006); P. I. Hurtado, J. Marro, and P. L. Garrido, Phys. Rev. E **74**, 050101 (2006).
[26] J.-H. Li and J. Łuczka, Phys. Rev. E **82**, 041104 (2010); A. A. Smirnov and A. L. Pankratov, Phys. Rev. B **82**, 132405 (2010); Z.-L. Jia and D.-C. Mei, J. Stat. Mech. (2011) P10010; M. Parker, A. Kamenev, and B. Meerson, Phys. Rev. Lett. **107**, 180603 (2011); D. Valenti, C. Guarcello, and B. Spagnolo, Phys. Rev. B **89**, 214510 (2014).
[27] J. Schuecker, M. Diesmann, and M. Helias, Phys. Rev. E **92**, 052119 (2015).
[28] A. O. Caldeira and A. J. Leggett, Ann. Phys. (N.Y.) **149**, 374 (1983).
[29] L. Magazzù, Ph.D. thesis, Palermo University, Palermo (2015).
[30] D. O. Harris, G. G. Engerholm, and W. D. Gwinn, J. Chem. Phys. **43**, 1515 (1965).
[31] J. C. Light and T. Carrington, *Discrete-Variable Representations and Their Utilization*, in *Advances in Chemical Physics* (Wiley, New York, 2007), Vol. 114, pp. 263–310.
[32] R. P. Feynman and F. L. Vernon, Jr., Ann. Phys. (N.Y.) **24**, 118 (1963).
[33] L. Magazzù, D. Valenti, B. Spagnolo, and M. Grifoni, Phys. Rev. E **92**, 032123 (2015); M. Grifoni, M. Sassetti, and U. Weiss, *ibid.* **53**, R2033 (1996).
[34] A. J. Leggett, S. Chakravarty, A. T. Dorsey, M. P. A. Fisher, A. Garg, and W. Zwerger, Rev. Mod. Phys. **59**, 1 (1987).
[35] V. V. Sargsyan, Y. V. Palchikov, Z. Kanokov, G. G. Adamian, and N. V. Antonenko, Phys. Rev. A **75**, 062115 (2007).
[36] P. Facchi, S. Tasaki, S. Pascazio, H. Nakazato, A. Tokuse, and D. A. Lidar, Phys. Rev. A **71**, 022302 (2005).
[37] K. W. Murch, U. Vool, D. Zhou, S. J. Weber, S. M. Girvin, and I. Siddiqi, Phys. Rev. Lett. **109**, 183602 (2012).
[38] F. Verstraete, M. M. Wolf, and J. I. Cirac, Nat. Phys. **5**, 633 (2009).
[39] K. Kechedzhi and V. N. Smelyanskiy, Phys. Rev. X **6**, 021028 (2016).